Novel hydrogen chemisorption properties of amorphous ceramic compounds consisting of p-block elements: exploring Lewis acid–base Al–N pair sites formed in situ within polymer-derived silicon–aluminum–nitrogen-based systems

Shotaro Tada, Norifumi Asakuma, Shiori Ando, Toru Asaka, Yusuke Daiko, Sawao Honda, Masaaki Haneda, Samuel Bernard, Ralf Riedel, Yuji Iwamoto

Novel hydrogen chemisorption properties of amorphous ceramic compounds consisting of p-block elements: exploring Lewis acid–base Al–N pair sites formed *in situ* within polymer-derived silicon–aluminum–nitrogen-based systems†

Shotaro Tada,[a] Norifumi Asakuma,[a] Shiori Ando,[a] Toru Asaka,[a] Yusuke Daiko,[a] Sawao Honda,[a] Masaaki Haneda,[a] Samuel Bernard,[b] Ralf Riedel[c] and Yuji Iwamoto[*a]

This paper reports the relationship between the H_2 chemisorption properties and reversible structural reorientation of the possible active sites around Al formed *in situ* within polymer-derived ceramics (PDCs) based on an amorphous silicon–aluminum–nitrogen (Si–Al–N) system. Al-modified polysilazane, as a ceramic precursor, was first pyrolyzed at 1000 °C under flowing ammonia to generate a Si–Al–N-based ceramic. XRD and HRTEM analyses confirmed the amorphous state of the titled ceramics. N_2 adsorption–desorption isotherm measurements and HAADF-STEM observation of amorphous SiAlN indicated that Al-incorporation in the early step of the process led to the generation of micro/mesoporosity in the amorphous ceramic with nanopores of 1 to 4 nm in size. XPS and pyridine sorption infra-red spectroscopy analyses revealed the *in situ* formation of Lewis acidic Al sites within the amorphous Si–Al–N surface network. As a result, the Si–Al–N compound was highly moisture sensitive. Then, to investigate the intrinsic properties of the highly reactive Al sites, the Si–Al–N compound was pretreated at 400–800 °C under an inert atmosphere. Temperature-programmed-desorption (TPD)-mass spectroscopy analysis of the pre-treated sample after H_2 treatment above 100 °C resulted in the detection of a broad H_2 desorption peak at around 100 to 350 °C. The H_2 desorption peak intensity apparently increased when H_2 treatment was performed at 150 °C, and the activation energy for H_2 desorption was determined to be 44 kJ mol^{-1}. ^{27}Al MAS NMR spectroscopic analysis for the pre-treated sample showed reversible local structure reorientation around reactive Al nuclei, and formation and deformation of 5-fold coordinated Al by H_2 chemisorption and desorption, respectively. In addition, the CO_2 hydrogenation reaction on the pre-treated sample was successfully demonstrated by TPD measurements after exposure to a mixed gas of H_2 and CO_2 with a 4 : 1 ratio at 400 °C. These results suggest that highly distorted 4-fold coordinated Al serves as a Lewis acid–base Al–N pair site to promote H_2 chemisorption at T > 100 °C followed by formation of a hydrogenated 5-coordinated Al unit where CO_2 hydrogenation proceeds at T ¼ 400 °C.

Introduction

The behavior of molecular hydrogen (H_2) on solid surfaces covers fundamental surface phenomena such as adsorption, diffusion, transformation, and desorption. In the simplest case, therefore, the main studies demonstrated the interactions of H_2 with solid surfaces in many chemical processes such as catalytic hydrogenation.[1–4]

For decades, the major system known to react with H_2 is transition metals (TMs)[1] because of their electronic properties which allow H_2 to easily adsorb and dissociate onto the metallic surface. TMs have partially occupied d-orbitals, which can accept σ electrons of H_2, while donating the d-electrons to the σ* antibonding orbital of H_2. Consequently, the H–H bond is weakened and cleaved—the so called homolytic dissociation of H_2. This paradigm shifted in 2006,[5,6] when a nonmetallic system was discovered to reversibly dissociate H_2 across Lewis acidic boron and Lewis basic phosphorous sites. Thereafter, similar

[a]*Department of Life Science and Applied Chemistry, Graduate School of Engineering, Nagoya Institute of Technology, Gokiso-cho, Showa-ku, Nagoya 466-8555, Japan*
[b]*University of Limoges, CNRS, IRCER, UMR 7315, F-87000, Limoges, France*
[c]*Institut für Materialwissenschaft, Technische Universität Darmstadt, Otto-Berndt-Str. 3, 64287 Darmstadt, Germany*

† Electronic supplementary information (ESI) available. See DOI: 10.1039/d0ta10271g

reactions were reported as a system called "Frustrated Lewis Pairs (FLPs)" that were derived from simple combination of electron donors and acceptors in which steric demands precluded the Lewis acid–base adduct.[6] According to a theoretical study on $PR_3/B(C_6F_5)_3$ pairs (R ¼ *t*Bu and $C_6H_2Me_3$),[7] the reaction between FLPs and H_2 starts *via* the polarization of a H_2 molecule induced by coordination of a H_2 molecule along the B–P axis between FLPs. Molecular H_2 polarization along FLPs occurs in the direction of P ◢ B ($P/H^{d+}/H^{d-}/B$). The binary polarization effect is associated with the reduction of the repulsion forces on both sides of the H_2 molecule. Electron transfer occurs through simultaneous P ◢ s*(H_2) and s(H_2) ◢ B donation in a push–pull manner and implies a progressive weakening of the H–H bond and following heterolytic H_2 dissociation into a proton (H^+) and hydride ion (H^-). In addition, as an extreme case of hydrogen chemisorption on inorganic compounds consisting of p-block elements, H_2 dissociation adsorption by III–V nanostructured materials in the form of nanosheets and nanotubes has been predicted for novel hydrogen storage materials.[8–12] Indeed, group III–V of nanostructured materials—an unsaturated electron-deficient group III element (electron acceptor site) and an electron-rich group V element (electron donor site)—can be categorized as Lewis acid–base components. Thus, heterolytic H_2 dissociation and adsorption occur in the same manner as in the FLP case. In particular, nanostructured aluminum nitride (AlN) materials have been suggested mainly theoretically as attractive compounds to offer a specific active site for the polarization of a H_2 molecule on the materials surface and subsequent heterolytic dissociation into H^+/H^- pairs.

Through a precursor route called polymer-derived ceramics (PDCs),[13–22] we recently demonstrated[19] the *in situ* growth of nanostructured AlN into a robust, protecting silicon carbide (SiC) matrix to form amorphous single-phase Si–Al–C–N ceramics at low temperatures and an AlN/SiC solid solution at high temperatures. By changing the nature of the atmosphere (ammonia instead of nitrogen) and considering the same commercially available poly(vinylmethyl-*co*-methyl)silazane (Durazane® 1800, silicon nitride precursor) chemically cross- linked with *N*,*N*-dimethylethylaminealane ($EtNMe_2$\$$AlH_3$), we have designed a novel amorphous single-phase ceramic based on the Si–Al–N system at low temperatures. This inorganic compound consisting of p-block elements has been character- ized in detail. Then, we demonstrate that it displays reversible H_2 adsorption–desorption properties governed by a possible Lewis acid–base pair site formed *in situ* within the amorphous surface network. Thus, the active acid sites of the amorphous surface network were investigated by X-ray photoelectron spectroscopy (XPS) and infra-red spectroscopy analyses whereas the H_2 adsorption and desorption behavior on polymer-derived amorphous SiAlN was investigated by measuring a profile of temperature-programmed desorption of hydrogen (H_2-TPD). The local molecular structure was monitored in detail by ^{27}Al solid-state magic-angle spinning Nuclear Magnetic Resonance (MAS NMR) before and after H_2 treatment. In addition, for further proof of the hydrogen chemisorption properties of this ceramic, CO_2-hydrogenation reactions were demonstrated by TPD measurements.

Experimental procedure

Synthesis of polymer-derived SiAlN ceramics

As previously reported by our groups,[19] a single-source precursor was first synthesized by chemical modification of commercially available Durazane® 1800, poly(vinylmethyl-*co*-methyl)silazane (PSZ, Merck KGaA, Darmstadt, Germany) with alane *N*,*N*-dimethylethylamine ($EtNMe_2$\$$AlH_3$—ADMEA, 0.5 M in toluene, Sigma-Aldrich Japan, Tokyo, Japan). The reaction of PSZ and ADMEA relies on both dehydrocoupling and hydroalumination reactions (Fig. S1†). For the present investigations, we applied a nominal atomic Al/Si ratio of 0.33 corresponding to a molar ratio between the monomeric units of ADMEA and PSZ. The handling of the chemicals and reagents was performed under an inert atmosphere of pure argon (Ar) using standard Schlenk techniques and vacuum/Ar lines. PSZ (4 mL, 63 mmol) was dissolved in 16 mL of anhydrous toluene at room temperature followed by cooling down to 0 °C. Then, 42 mL (21 mmol) of ADMEA was added dropwise to the PSZ solution under stirring. When the addition was completed, the temperature was naturally increased up to room temperature and the stirring was continued for 24 h. Then, the solvent was distilled off under vacuum at 60 °C to afford Al-modified PSZ (Al-PSZ).

Chemical modification performed in this study was moni- tored by attenuated total reflection Fourier transform infra-red (ATR-FTIR) spectroscopy using a FTIR spectrometer (FT/IR- 4200IF, JASCO Corporation, Tokyo, Japan) with attachment of ATR equipment (ATR PRO 550S-S/570S-H, JASCO Corporation, Tokyo, Japan) at a resolution of 4 cm^{-1}. The typical ATR-FTIR spectra of Al-PSZ samples with different Al/Si atomic ratios shown in Fig. S2† indicate that both hydroalumination and dehydrocoupling reactions occur.

Al-PSZ was placed in a quartz crucible loaded in a quartz tube in which atmospheric conditions can be varied between NH_3 and N_2 gasses during pyrolysis. Then, the synthesized single source precursor was pyrolyzed to afford a SiAlN ceramic material under an NH_3 flow at 1000 °C for 2 h with a heating rate of 3 °C min^{-1} and subsequently flushed with N_2 and cooled down to room temperature with the same rate of 3 °C min^{-1}. The as-pyrolyzed samples are labelled SiAlN. According to the same pyrolysis route, a reference sample free of aluminum and derived from as-received PSZ was prepared. It is labelled SiN.

Characterization techniques

Transmission electron microscope (TEM) observations and high-angle annular dark-field-scanning transmission microscope (HAADF-STEM) observations were performed on the as-pyrolyzed SiAlN sample using an atomic-resolution analytical microscope, JEOL JEM-ARM200F (JEOL Ltd., Tokyo, Japan) operated at an accelerating voltage of 200 kV.

The powder X-ray diffraction (XRD) patterns of the pyrolyzed samples were measured on a flat sample stage, using Ni-filtered

CuKa radiation (Model X'pert, Philips, Amsterdam, The Netherlands).

The textural properties of the pyrolyzed samples were evaluated by measuring N_2 adsorption and desorption isotherms at —196 °C under relative pressures ranging from 0 to 0.99 (Model Belsorp Max, BEL Japan Inc., Osaka, Japan). The pore size distribution was analyzed by MP[23] and BJH[24] methods. H_2 adsorption–desorption measurements at —193 °C were performed by the same outgassing procedure mentioned for N_2 adsorption–desorption isotherm measurements as described above. As reference samples, commercially available crystalline AlN (99.9%, Kojundo Chemical Laboratory Co.,Ltd., Japan) and zeolite (type HY, HSZ-320HOA, Tosoh Co., Ltd., Tokyo, Japan) were evaluated in the same manner.

The chemical composition of the pyrolyzed samples was determined as follows:

$$\text{wt\%(Si + Al)} = 100\% - \text{wt\%(C)} - \text{wt\%(O)} - \text{wt\%(N)} \quad (1)$$

The carbon content was analyzed using a carbon analyzer (non-dispersive infrared method, Model CS844, LECO Corporation, Michigan, USA); the oxygen and nitrogen contents were measured using an oxygen nitrogen hydrogen analyzer (inert-gas fusion method, Model EMGA-930, HORIBA, Ltd., Kyoto, Japan). The Al/Si ratio was determined using an energy dispersive X-ray spectrometer (EDS, Model JSM-6010LA, JEOL Ltd., Tokyo, Japan) mounted on a scanning electron microscope (SEM, Model JSM-6010LA, JEOL Ltd., Tokyo, Japan). The chemical compositions of the pyrolyzed samples are listed in Table 1.

To investigate the chemical bonding-state of the SiAlN sample, X-ray photoelectron spectroscopic (XPS) measurements were performed using an X-ray Photoelectron Spectrometer (PHI 5000, ULVAC-PHI, Inc., Japan) with an Al Ka X-ray source operated at 14 kV and 14 mA. An alignment on the C 1s peak was performed before survey scans. Deconvolution of each spectrum was performed using the Igor pro 7 fitting engine. A program package of X-ray Photoelectron Spectroscopy Tools (XPST) was used in this study. Non-linear curve-fittings were performed using the Pseudo-Voigt function[25] with a Gauss-Lorentz ratio of 0.3.

To investigate the surface bonding nature of the SiAlN sample, diffuse reflectance infrared Fourier transform (DRIFT) spectroscopic analysis was performed. The sample was diluted to 5 wt% by mixing with nano-diamonds (NDs, IRM 5-12, Tomei Diamond Co., Ltd, Tokyo, Japan). An alumina cup was filled with the diluted sample and loaded in the measurement chamber. DRIFT spectra were recorded at specific temperatures of 150, 250, 300, 350, 400, 450, 500, and 600 °C under flowing Ar. Pyridine adsorption was *in situ* monitored for the sample loaded in a potassium bromide (KBr) pellet by measuring FTIR spectra at a resolution of 4 cm^{-1} (Model JASCO FT/IR 4200, JASCO., Tokyo, Japan). The signal-to-noise ratio was improved by averaging 64 scans. Measurements were conducted by using a custom designed IR cell which allowed heat-treatment of the sample *in situ* as well as the introduction of various gasses and/or pyridine vapor through a precise valve system. Prior to the measurements, the SiAlN sample was maintained at 400 °C under vacuum. Then, pyridine sorption IR data were recorded after introduction of 10 Torr of pyridine vapor and subsequent removal of the vapor under vacuum at R.T.

Hydrogen adsorption and desorption properties of polymer-derived SiAlN ceramics

To study the H_2 adsorption and desorption properties, temperature-programmed-desorption of hydrogen (H_2-TPD) was performed using a catalyst analyzer (Model BELCAT-A, MicrotracBEL Corp., Osaka, Japan) fixed with a quadrupole mass spectrometer (Model BELMASS, MicrotracBEL Corp., Osaka, Japan). The setup of the career-gas flow was 50 cm^3 min^{-1}. 250 mg of sample was placed in a channel-shaped quartz tube with an initial diameter of 6 mm. The quartz tube was hermetically connected to the system with the aid of O- rings. Temperature-programmed heating was always managed with a thermocouple which was inserted to the bottom of the quartz tube. The SiAlN sample was maintained under Ar at 800 °C and subsequently exposed to pure H_2 for 5 min at specific temperatures (100 °C and 150 °C). After cooling to 50 °C, the gas was changed from H_2 to Ar and maintained for 60 min at 50 °C. The TPD-curve was recorded under Ar up to 600 °C with a heating rate of 5 °C min^{-1}.

The local structure around the Al atoms in the SiAlN sample before and after H_2 treatment at 150 °C was intensively studied by ^{27}Al solid-state MAS NMR spectroscopic analysis with a 600 MHz NMR spectrometer (Model JNM-ECA600II, JEOL Ltd., Tokyo, Japan) operating at a static magnetic field of 14.01 T (155.4 MHz). The diameter of the rotor used in the MAS probe was 3.2 mm. All experiments were performed at R.T. with a spinning rate of 20 kHz. The typical ^{27}Al resonance was acquired using a single pulse of 90° (1.2 ms width in this study) with a recycle delay of 2 s. Deconvolution of each spectrum was

Table 1 Chemical composition of 1000 °C-pyrolyzed samples

	Composition (wt%)					Composition (at%)
	EDS (Al/Si ratio)		Elemental analysis (wt%)			
Name	Si	Al	C	N	(O)	Atomic ratio to Si
SiN	65.0	0	1.6	32.5	0.9	$Si_1C_{0.06}N_{1.00}(O_{0.02})$
SiAlN	51.9	17.3	0.1	21.8	9.0	$Si_1Al_{0.35}N_{0.84}(O_{0.30})$

performed by using the Igor pro 7 fitting engine. Non-linear curve-fittings were carried out using the Lorentzian-type profile. For further proof of the presence of chemisorbed hydrogen on the SiAlN sample, TPD measurements were performed on the SiAlN sample after exposure to a mixed gas with a 4 : 1 molar ratio of H_2 and CO_2 or pure CO_2 at 400 °C for 60 min. The post-reaction TPD-MS profile of CO_2 (m/z ¼ 44) was recorded.

Results and discussion

General characterization of polymer-derived SiAlN

As shown in the XRD patterns presented in Fig. S3,† the pyrolysis of Al-modified PSZ under flowing NH_3 leads to an X-ray amorphous SiAlN sample. To investigate the nanostructure and the crystallinity of the SiAlN sample in more detail, TEM has been performed. The High-Resolution TEM (HRTEM) images depicted in Fig. 1a and b show contrast between adja- cent areas without grain boundaries while the selected area electron diffraction pattern (SAED) as the inset in Fig. 1b exhibits a typical amorphous halo pattern, which highlights the conclusions made by X-ray diffraction. For further analysis of the observed contrasts shown in Fig. 1a, scanning TEM imaging (STEM) has been conducted (Fig. 1c and d). The spot with bright contrast observed in the bright-field (BF) image (Fig. 1c) turned to black spots in the dark-field (DF) mode with High Angle Annular Dark Field detector—HAADF (Fig. 1d). Thus, the line scanning result for the selected spot with relatively clear dark contrast in the DF-image (Fig. 1d) indicates the presence of voids of approximately 3.3 nm in diameter size as shown Fig. 1e.

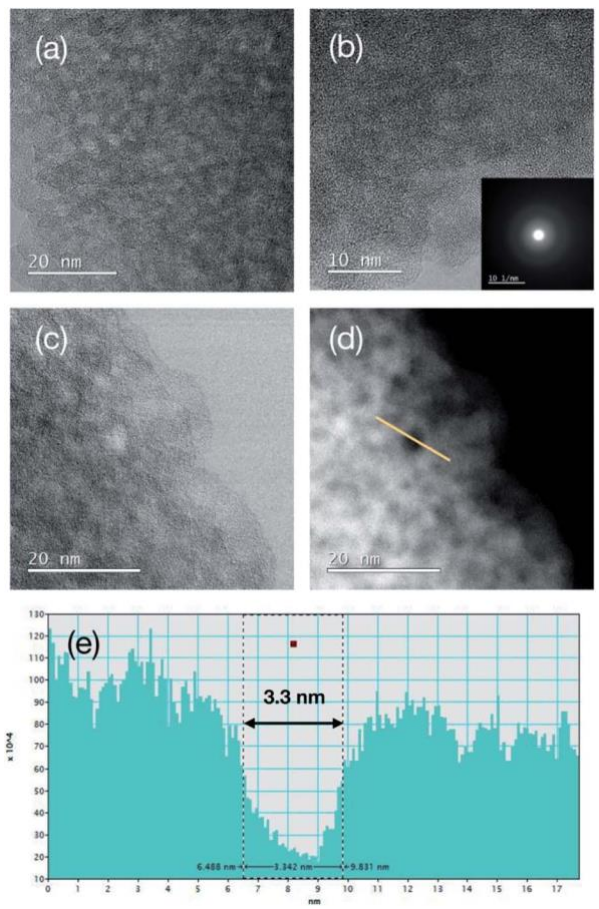

Fig. 1 TEM observation of polymer-derived amorphous SiAlN. (a) HRTEM image, (b) high magnification TEM image and the corresponding SAED pattern obtained, (c) BF-STEM image, (d) HAADF-STEM image and (e) line scanning result for the spot with dark contrast in (d).

To confirm the presence of pores in the sample, we have investigated porosity at the micro and mesoscopic length scale by N_2 adsorption–desorption isotherm measurements at —196 °C. As reference data, the SiN sample and another SiAlN sample which was pyrolyzed under flowing N_2 at 1000 °C (labelled SiAlN@N_2) have been investigated for comparison. The results are shown in Fig. S4 and S5.† The SiAlN sample at —196 °C exhibited a type I + IV isotherm according to the IUPAC classifications,[26,27] while the SiN (Fig. S4a†) and SiAlN@N_2 samples (Fig. S5a†) showed no interaction with N_2. The Brunauer–Emmett–Teller (BET) surface area ($S_{BET}^{N_2}$) of the SiAlN sample has been measured to be 165 m^2 g^{-1}. The pore size distribution curve (PSD) in the micropore range characterized by the MP method[19] exhibited a peak centered at 1.2 nm (Fig. S4b†), whereas there was no distinct peak in the mesopore range in the BJH plot[24] although we can identify the existence of a certain porosity with a pore size range of approximately 2 to 4 nm (Fig. S4c†). This is consistent with the observed mesopores in the STEM images and this highlights that the SiAlN sample displays bimodal porosity which is expected to offer molecular reactivity through diffusion or dispersion phenomena.

It is generally recognized that the formation of micro/mesopores in PDCs is due to the release of gaseous by- products during the polymer-to-ceramic conversion process because of reactions such as transamination, condensation and dehydrocoupling reactions. However, such micro-/meso-porosity—which is formed *in situ*—is in general unstable in the high temperature regime of the polymer-to-ceramic conversion, *i.e.*, 700–800 °C, and therefore collapses.[28] This is why the SiN sample—formed by pyrolysis of PSZ at 1000 °C under NH_3—is nonporous (Fig. S4a†). In contrast, it turns out that micro/mesoporosity stays stable in the SiAlN sample in the tempera- ture range of 700–1000 °C under flowing NH_3 (Fig. S4 and S5b†) most probably because reactions still occur in the high temperature regime of the polymer-to-ceramic conversion, *e.g.*, reactions of the SiAlN samples with hydrogen which is gener- ated by dissociation of NH_3, *i.e.*, partial cleavage of the amor- phous network. This is confirmed through TG experiments which have been performed under flowing NH_3–N_2 (at a flowratio of 60 : 40) mixed gas and He. The results are shown in Fig. S6 and S7,† respectively. A continuous weight loss above 700 °C was identified during the conversion of Al-modified PSZ under the NH_3–N_2 gas flow leading to the SiAlN sample whereas no weight loss is identified above 800 °C during the conversion of PSZ into the SiN sample (Fig. S6†). In addition, such a difference above 800 °C was not observed when the conversions of Al-modified PSZ and PSZ were monitored under He (Fig. S7†). Indeed, SiAlN@N_2 was nonporous (Fig. S5a†). Therefore, micro/mesoporosity formation was governed by the

reaction with hydrogen derived formed *in situ* due to the thermal decomposition of NH_3.

Table 1 lists the chemical composition of the as-pyrolyzed samples. The measured Al/Si atomic ratio of the SiAlN sample is 0.35 which is consistent with the nominal atomic Al/Si ratio of 0.33 fixed at the polymer level. In addition, the residual carbon content in the SiAlN sample is as low as 0.1 wt% because of the use of an NH_3 atmosphere,[29] while the oxygen content is relatively high (9.0 wt%) most probably because of the general procedure of elemental analyses in air for a few minutes.

The bonding nature at the surface of the SiAlN sample was assessed by XPS analysis. The wide scan spectrum of SiAlN sample is shown in Fig. S8.† Besides the intense lines of the constituent elements (N 1s, Si 2p and Al 2p) and unavoidable carbon contaminant, the strong line of O 1s is observed. This indicates that a certain amount of oxygen is present at the surface of the SiAlN sample. Fig. 2a and b show the high- resolution Si 2p and Al 2p peaks, respectively. The deconvolu- tion of the Si 2p spectrum (Fig. 2a) yields a major peak at 101.6 eV and a minor peak at 103.2 eV assigned to Si–N and Si–O bonds, respectively.[30,31] The deconvolution of the Al 2p spectrum (Fig. 2b) also yields two peaks at 73.6 and 74.4 eV assigned to Al–N and Al–O bonds, respectively.[32] However, the relative peak area ratio A_{Al-O}/A_{Al-N} is much higher than A_{Si-O}/A_{Si-N} in the Si 2p spectrum as shown in Table S1.†

To identify the origin of the oxygen contaminant in more detail, diffuse reflectance infrared Fourier transform (DRIFT) spectroscopic analysis was performed. The typical DRIFT spectra of the SiAlN sample recorded at different temperatures

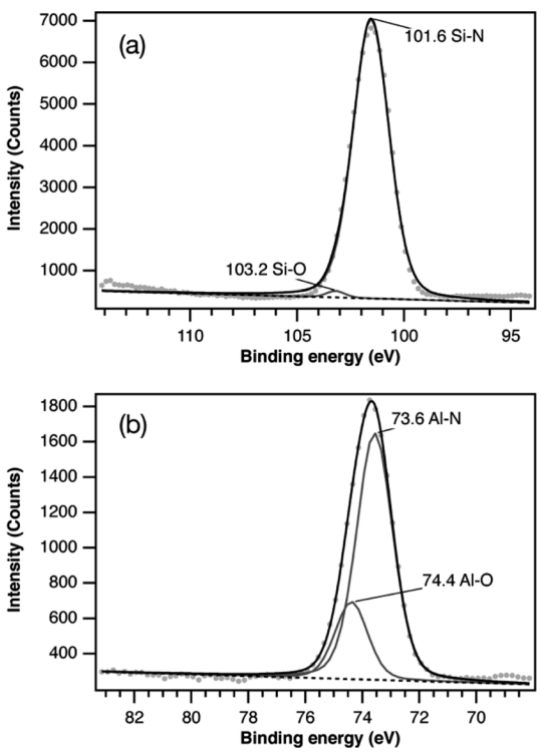

Fig. 2 High-resolution X-ray photoelectron spectra of amorphous SiAlN: (a) Si 2p and (b) Al 2p line.

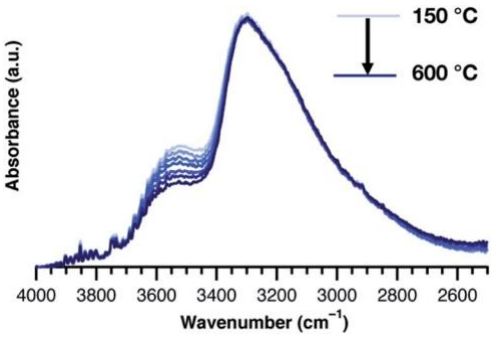

Fig. 3 DRIFT spectra for amorphous SiAlN recorded at specific temperatures ranging from 150 to 600 °C under Ar.

under an Ar flow are shown in Fig. 3. The SiAlN sample exhibits broad absorption bands around 3550 cm^{-1} (nO–H) and 3300 cm^{-1} (nN–H). With increasing temperature from 150 to 600 °C, the absorption band intensity around 3550 cm^{-1} apparently decreases. Accordingly, the absorption band around 3550 cm^{-1} is attributed to the O–H groups of chemisorbed water. These results revealed, in addition to the presence of a certain form of porosity, the existence of a certain number of highly reactive Al sites which can be easily occupied by water molecules under ambient moisture conditions. Based on the high reactivity of Al sites formed *in situ* within the amorphous SiAlN surface, we used pyridine as a probe molecule for the quantitative analysis of the surface acidity of the SiAlN sample by FTIR spectroscopy. Prior to the measurements, the SiAlN sample was pre-treated at 400 °C under vacuum to remove the chemisorbed water. The differential spectrum after pyridine adsorption on the pre-treated SiAlN sample at R.T. is presented in Fig. 4. It highlights the characteristic bands attributed to pyridine coordinated on Lewis acid sites (Py-L) at 1629 and 1455 cm^{-1},[33] thus revealing that the highly reactive Al sites in the SiAlN sample work as surface Lewis acid sites. As a consequence, we suggested that Al sites located at the surface of the SiAlN sample are expected to serve as preferential chemisorption sites for gas molecules such as hydrogen molecules (H_2) as

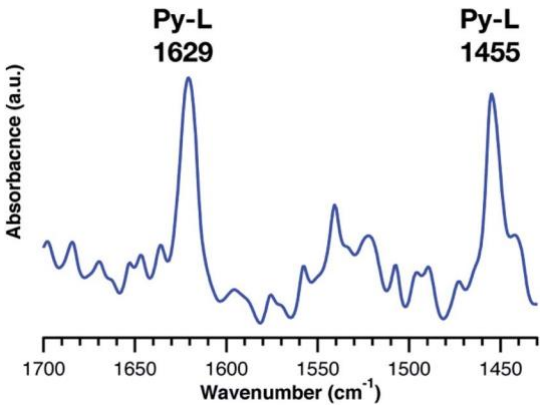

Fig. 4 Differential FT-IR spectrum of the pre-treated SiAlN sample after pyridine adsorption at room temperature.

predicted for nanostructured AlN.[8–12] Before the investigation, a pre-treatment step was performed on the SiAlN sample by heat-treatment under an inert atmosphere at a sufficiently high temperature of 400–800 °C to allow removing the chemisorbed water from the sample surface. The pre-treated SiAlN sample is labelled PTSiAlN.

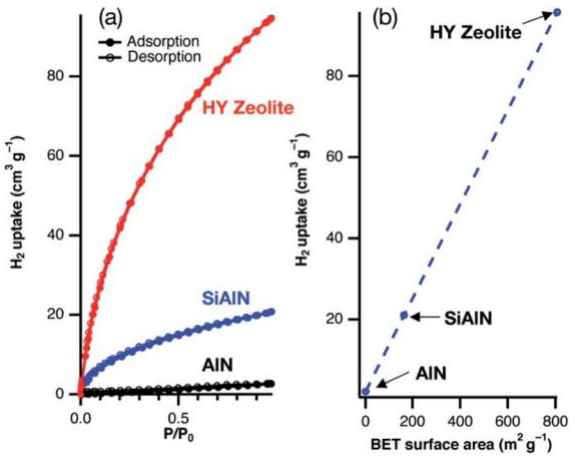

Fig. 5 (a) Volumetric H_2 adsorption and desorption isotherms at —193 °C for PTSiAlN and commercially available crystalline AlN and zeolite samples. (b) The correlation between the H_2 uptake and measured BET surface area.

Hydrogen adsorption and desorption properties of polymer-derived SiAlN

At first, volumetric H_2 adsorption and desorption isotherms at —193 °C of the PTSiAlN sample were recorded over the relative pressure range of 0 to 0.99, and compared with those of commercially available crystalline AlN ðmeasured $S_{BET}^{N_2}$ ¼ 3:3 $m^2\ g^{-1}$Þ and zeolite (type HY, measured $S_{BET}^{N_2}$ ¼ 807 $m^2\ g^{-1}$) (Fig. 5a). The H_2 adsorption–desorption at —193 °C of the PTSiAlN sample is fully reversible. In addition, the H_2 uptake at 1 atm increases along with the BET surface areas of the PTSiAlN sample and reference samples (Fig. 5b). These results indicate that the PTSiAlN sample exhibits typical H_2 physisorption behavior at —193 °C. Then, temperature-programmed-desorption of hydrogen (H_2-TPD) was performed on the PTSiAlN sample to study the hydrogen chemisorption properties. Prior to the measurements, the PTSiAlN sample was maintained under Ar at 800 °C and subsequently exposed to H_2 at specific temperatures (T_{H2} ¼ 100, 150 °C) for 5 min (labelled H_2PTSiAlN sample). The typical H_2-TPD profiles of the

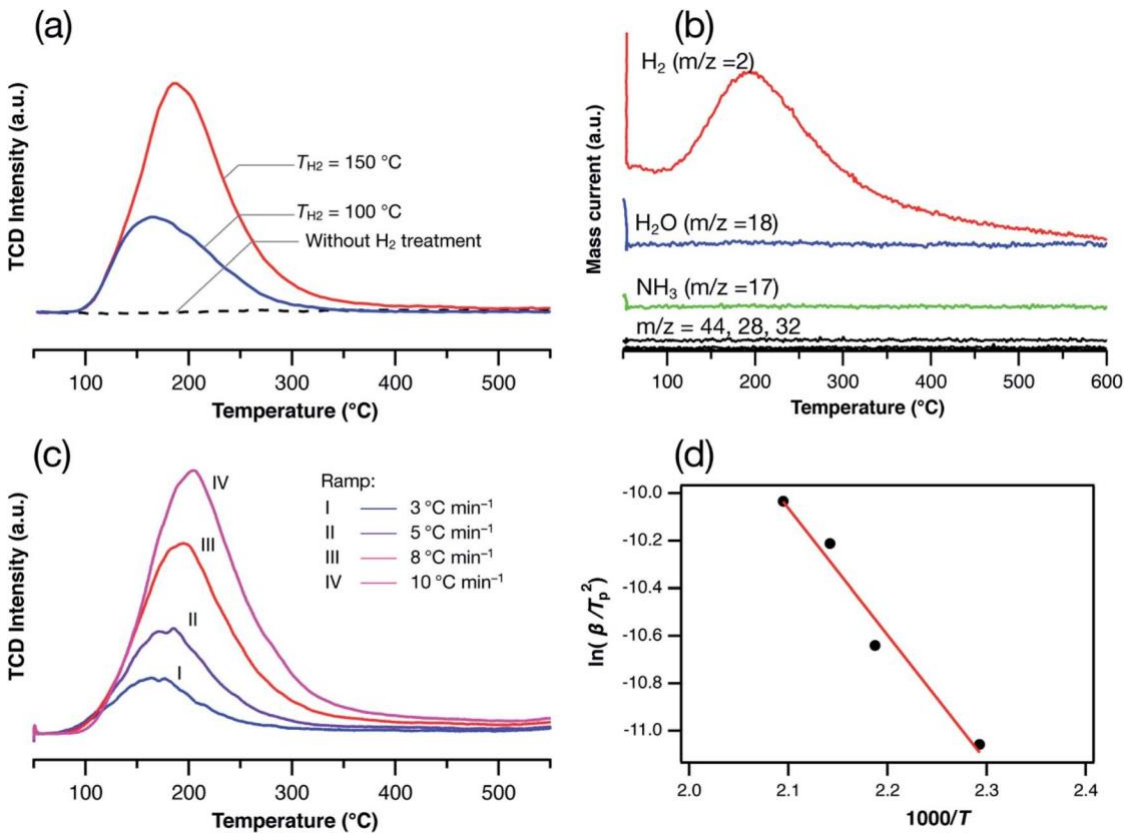

Fig. 6 (a) H_2-TPD profiles for the PTSiAlN sample: blue and red solid lines represent H_2 exposure temperatures (T_{H2}) of 100 and 150 °C for 5 min, respectively. The dashed line represents the TPD profile without H_2 treatment. (b) H_2-TPD mass profiles for PTSiAlN after H_2 exposure at 150 °C for 5 min. (c) Variation of the H_2-TPD profiles for the sample after H_2 exposure at 150 °C by varying the temperature ramping rate b from 3 to 10 °C. (d) Plot of $\ln(b/T_{Peak}^2)$ against $1000/T_{Peak}$. The activation energy for H_2-desorption was estimated from the slope of the straight line (44 kJ mol^{-1}).

H_2PTSiAlN samples are shown in Fig. 6a. The H_2-TPD profile after the H_2-treatment at 100 °C (T_{H2} ¼ 100 °C) exhibits a single peak at approximately 100 to 350 °C. The peak intensity apparently increases for H_2-treatment performed at 150 °C (T_{H2} ¼ 150 °C) whereas no peaks were detected without H_2 exposure (PTSiAlN sample, black-line in Fig. 6a). Simultaneous *in situ* mass analysis during peak detection (Fig. 6b) confirmed the presence of a single desorbed H_2 component. It should be noted that the H_2-TPD profiles of reference samples, *i.e.*, commercial crystalline AlN and HY zeolite samples (Fig. S9†), show no desorption peak under the same measurement conditions (T_{H2} ¼ 150 °C). The activation energy for H_2 desorption was estimated by Redhead analysis: the activation energy for desorption of component *i* ($DE_{d,i}$) can be calculated from the slope of the straight line obtained by plotting $\ln(b/T_p^2)$ *vs.* $1/T_p$ where b and T_p are the temperature ramping rate and absolute peak temperature, respectively.[34,35] In this study, T_{H2} ¼ 150 °C was applied, and the H_2-TPD profiles were measured by varying b from 3 to 10 °C min^{-1} (Fig. 6c). Both the H_2 desorption peak intensity and T_p increase consistently with b, and the resulting plot successfully provides a straight line with a specific slope to give $DE_{d,H2}$ of 44 kJ mol^{-1} (Fig. 6d) which is sufficiently high to be assigned as hydrogen chemisorption.

To understand such a behavior, the local structure around the Al atoms in the PTSiAlN sample before (PTSiAlN) and after (H_2PTSiAlN) H_2 treatment at 150 °C was studied by ^{27}Al solid-state MAS NMR spectroscopy. The ^{27}Al MAS NMR spectra are recorded for the PTSiAlN sample stepwise after each treatment as follows: the PTSiAlN sample is exposed to H_2 at 150 °C for 6 h (H_2PTSiAlN sample), and then the H_2PTSiAlN sample is post heat-treated at 450 °C for 1 h under Ar (labelled H_2PTSiAlNAr). The ^{27}Al MAS NMR signal in the spectrum of the PTSiAlN sample is shown in Fig. 7a. The deconvolution of the broad ^{27}Al MAS NMR signal provides major signals around 95 and 65 ppm assigned to distorted tetrahedral Al (Al_{IV}) units[36,37] represented as $AlN_{4-x}L_x$ (L ¼ N, O and H, *x* ¼ 1–3), and five-fold coordinated Al (Al_V) units[36,38,39] represented as $AlN_{5-x}L_x$ (*x* ¼ 1–4), respectively. Minor signals detected around 35 and 6 ppm are assigned to highly distorted octahedral Al (Al_{VI}) units and normal Al_{VI} units, respectively.[36] By comparing the spectra of the PTSiAlN and H_2PTSiAlN samples (Fig. 7b), the relative intensity of the signal around 65 ppm apparently increases (red signal) compared to the initial one (black signal). Then, after post-treatment under Ar at 450 °C for 1 h (H_2PTSiAlNAr sample), the relative intensity of the blue signal around 65 ppm is observed to decrease in the spectrum of the H_2PTSiAlNAr sample to an intensity close to that of the black signal. The increase in the signal intensity around 65 ppm after H_2 treatment at 150 °C (H_2PTSiAl sample) clearly indicates the chemical interaction of the guest molecules with Al. Then, the decrease of the peak around 65 ppm after the post-treatment at 450 °C (H_2PTSiAlNAr sample) indicates the desorption of guest molecules chemisorbed to Al. This behavior is in good agreement with the H_2-desorption behavior in H_2-TPD profiles described above. The changes of the line-shape in the ^{27}Al MAS NMR spectra and the H_2-TPD profiles suggest that occurrence of reversible local structure reorientation around active Al nuclei,

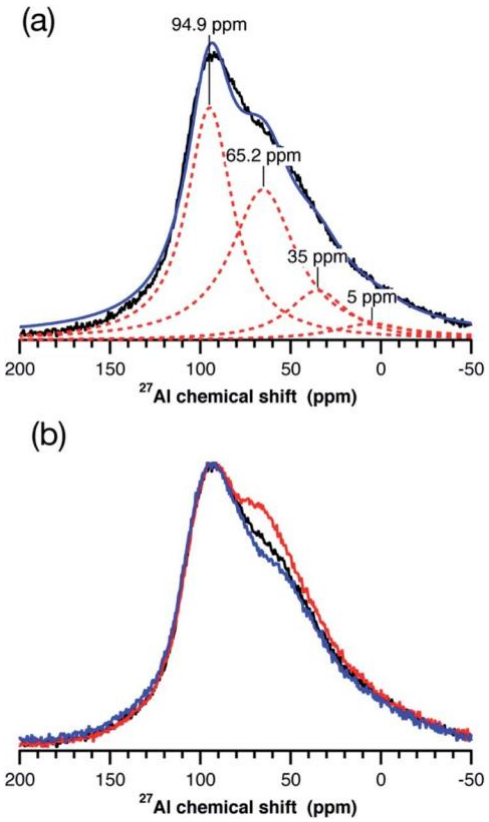

Fig. 7 (a) A typical ^{27}Al MAS NMR spectrum of the PTSiAlN sample. The black line represents experimental data, the blue line represents curve-fitting results indicated by Lorentzian curves and the red dashed line represents sub-peaks. (b) ^{27}Al MAS NMR spectra recorded for PTSiAlN stepwise after each treatment as follows: The PTSiAlN sample (Black line) was exposed to H_2 at 150 °C for 6 h (H_2PTSiAlN sample, Red line), and then H_2PTSiAlN was post heat-treated at 450 °C for 1 h under Ar (Blue line).

and formation and deformation of Al_V units, by adsorption and desorption of H_2 gas molecules, respectively. The formation of Al_V units in H_2PTSiAlN indicates that 5-fold coordinated local structure formation is more favorable.

In the case of crystalline AlN, the ^{27}Al MAS NMR spectrum exhibits a sharp signal near 110 ppm (ref. 35) due to the highly symmetric AlN_4 unit consisting of three covalent bonds together with one dative bond formed as a Lewis acid–base adduct (sp_3 hybridization). Thus, there is no site for H_2 chemisorption on the crystalline AlN. In addition, the peak intensity of the Al_{IV} units at 95 ppm after H_2 treatment has not changed at all (Fig. 7b). Thus, these fully occupied tetrahedral sites detected for the crystalline AlN and PTSiAlN samples do not serve as H_2 chemisorption sites. Moreover, the signal peak intensity of the Al_{IV} units around 35 and 6 ppm has not changed after the H_2 treatment. These results indicate that the preferential H_2 chemisorption sites of the PTSiAlN are undetectable by ^{27}Al MAS NMR spectroscopy.

As reported previously,[40] Al sites with a strong distortion of the symmetry are "NMR-invisible". The preferential H_2 chemisorption sites are thought to be H_2-accesible

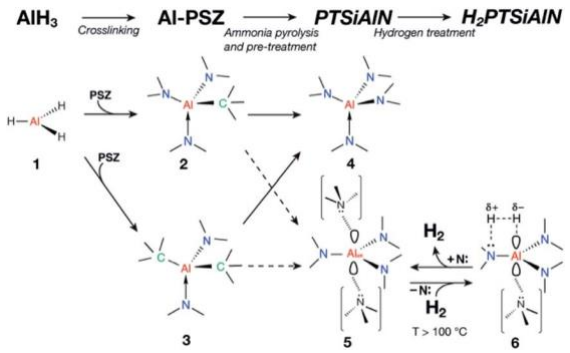

Fig. 8 Proposed scheme for the formation of Al_V units by the hydrogenation of Al_{un} units.

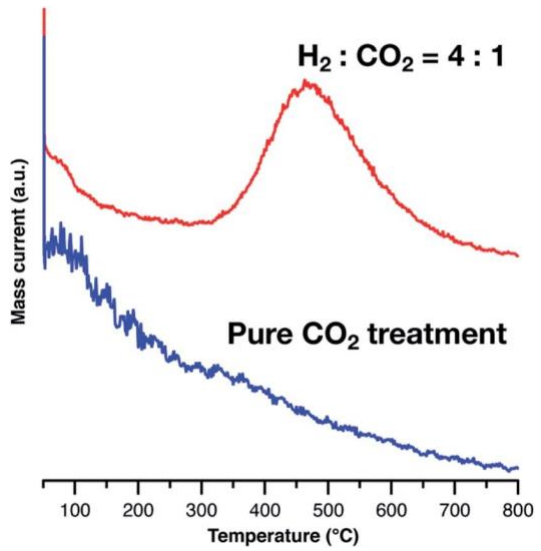

Fig. 9 Post reaction TPD-MS profiles of CO_2 (m/z 44) under an Ar flow. The measurements were performed after exposure to a mixed gas with a 4 : 1 molar ratio of H_2 and CO_2 (Red) and pure CO_2 at 400 °C (Blue).

unoccupied asymmetric sites having the coordination number lower than 4. In addition, the Al sites are intensively distorted compared with the NMR-visible Al_x units (x = IV, V and VI), and thus preferentially stabilized *via* H_2-chemisorp- tion to form Al_V units.

As one possible highly distorted unoccupied site (denoted as Al_{un}), we suggest a pseudo three-coordinated Al site stabilized by weekly coordinated two N^ ligands within the SiAlN amorphous network shown in the following proposed reaction scheme for H_2 chemisorption (Fig. 8): the starting coordination of Al as a monomer precursor is three-coordinated (Fig. 8, **1**). After the chemical modification of PSZ with **1** followed by crosslinking of the polymer network, the Al in Al-PSZ is converted to mainly 4-fold coordination to afford mixed $AlN_{4-x}C_x$ (x = 1, 2) tetrahedral units *via* hydroalumination as well as dehydrocoupling reactions (Fig. 8, **2** as AlN_3C and **3** as AlN_2C_2).[19] Then, the pyrolysis under NH_3 up to 1000 °C leads to the formation of distorted Al_{IV} units (Fig. 8, **4**) accompanied by a certain fraction of unoccupied Al_{un} units (Fig. 8, **5**) due to Al–C bond cleavage by the hydrogen formed *in situ* above 500 °C under an NH_3 flow as discussed above. The fraction of Al_{un} units in PTSiAlN served as a Lewis acid site to give Al_V units *via* the coordination of nucleophiles such as H_2O or pyridine (sp^2p_z hybridization[41,42]), which is observed at 65 ppm in Fig. 7a. In addition, H_2 chemisorption at T > 100 °C detected by H_2-TPD analysis was thought to be promoted by the Lewis acid–base Al–N pair site in a push–pull manner analogous to that of FLPs as mentioned above: molecular H_2 polarization starts on a partially unoccupied p_z orbital of Al_{un} and sp^3 lone pair of nitrogen. This promotes electron transfer through simultaneous $\sigma(H_2)$ → Al and N → $\sigma^*(H_2)$ and donation in a push–pull manner implying a progressive weakening of the H–H bond, which results in the formation of the hydrogenated Al unit having 5-fold coordination (Fig. 8, **6**).

According to a previous report on the DFT calculations for H_2 adsorption on nanostructured AlN, the energy barrier between the initial state and transition state of the H_2 molecule was estimated to be 86 kJ mol^{-1}, while the one for transition from physisorption to chemisorption of the H_2 molecule was −10.6 kJ mol^{-1}.[12] The $\Delta E_{d,H2}$ of the H_2PTSiAlN sample (44 kJ mol^{-1}) in this study is lower than the one predicted for nanostructured AlN (approximately 97 kJ mol^{-1}). This was thought to be explained by the following difference in the chemical bond formations as discussed above: the nanostructured AlN is predicted to form an Al_{IV} unit (sp^3 hybridization) *via* the strong Al–H and N–H σ-bond formations,[12] whereas the SiAlN sample is suggested to form an Al_V unit (sp^2p_z hybridization) *i.e.* formation of a slightly elongated and weak hydrogenated structure along the p_z axis as **6** in Fig. 8.[41,42]

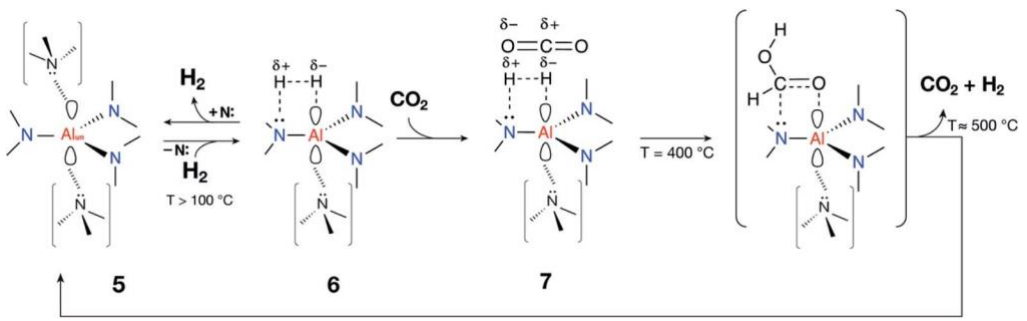

Fig. 10 Possible reaction scheme for CO_2 hydrogenation on polymer-derived amorphous SiAlN.

For further experimental proof of the presence of chem- isorbed hydrogen on the SiAlN sample, the CO_2 hydrogenation reaction on the PTSiAlN sample was demonstrated by TPD measurements after exposure to a mixed gas with a 4 : 1 molar ratio of H_2 and CO_2 or pure CO_2 at 400 °C. The post-reaction TPD-MS profiles of CO_2 (m/z ¼ 44) are shown in Fig. 9. The TPD-MS profile after pure CO_2 treatment exhibits a very weak and broad peak around 100 °C. In contrast, the profile after the H_2–CO_2 mixed gas treatment exhibits a broad but distinct CO_2 desorption peak from 350 to 650 °C. The temperature range above 300 °C found for CO_2 desorption corresponds to the re- ported thermal decomposition of formic acid (HCOOH) or formate ($HCOO^-$) to release CO_2 and H_2.[43,44] Fig. 10 shows a possible reaction scheme for CO_2 hydrogenation. As discussed above, the exposure of the PTSiAlN sample to H_2 leads to the formation of H_2PTSiAlN (6) which can be coordinated with CO_2 *via* the dipole-induced dipole interaction to give the adduct intermediate H_2 (7). Then, CO_2 hydrogenation proceeds to yield HCOO(H) which subsequently decomposes to release CO_2 and H_2 at T ~ 500 °C.

Conclusions

In this study, an inorganic compound consisting of p-block elements, namely silicon, aluminum and nitrogen elements distributed within an amorphous network and displaying novel hydrogen chemisorption properties was synthesized by pyrolysis of aluminum-modified polysilazane as a ceramic precursor at 1000 °C under flowing NH_3. We experimentally demonstrated the relationship between the H_2 chemisorption properties and structural reorientation of the active Al sites formed *in situ* within the polymer-derived amorphous SiAlN surface network. The results can be summarized as follows:

1. HRTEM and STEM analyses and N_2 adsorption–desorption isotherm measurements at —196 °C revealed micro/mesoporosity formation in the SiAlN sample in the high temperature regime of pyrolysis (700–1000 °C) under NH_3.

2. Chemical composition analyses, DRIFTS and XPS measurements revealed that the incorporation of Al into the amorphous silicon nitride matrix resulted in the formation of Lewis acidic Al characterized by pyridine sorption FTIR.

3. H_2-TPD measurements revealed the unique reversible H_2 adsorption and desorption properties of the titled compound. The measured activation energy for H_2-desorption ($DE_{d,H2}$) was approximately 44 kJ mol^{-1}, which was sufficiently high to be assigned as hydrogen chemisorption.

4. Reversible H_2 chemisorption and desorption were successfully identified by ^{27}Al MAS NMR spectroscopic analyses: the results strongly suggested that local structural reorientation reversibly occurs between undetectable highly distorted Al sites and clearly detectable Al_V units by H_2 adsorption and desorption.

5. The highly distorted Al sites served as a Lewis acid–base Al–N pair site which was suggested as a possible H_2 chemisorption site, and a pseudo three-coordinated Al site was proposed for the one possible H_2 chemisorption site.

6. CO_2 hydrogenation on the amorphous SiAlN sample surface was successfully demonstrated by TPD measurements after sample exposure to a mixed gas with a 4 : 1 ratio of H_2 and CO_2 at 400 °C. The results are clear evidence that H_2 chemisorbed on the Lewis acid–base Al–N pair site.

There is still room for further study on optimizing hydrogen adsorption–desorption properties by controlling several material parameters such as the chemical composition and micro/mesoporosity. Moreover, the unique H_2-affinity of present SiAlN suggests other applications such as a novel non-oxide catalysis support which is recently highlighted for the impressive catalytic activities in hydrogenation of polymer derived transition metal/Si-based non-oxide ceramic nanocomposites of palladium silicide containing SiCN by Motz and Kempe *et al.*,[20] and Ni-SiOC by Wilhelm and Rezwana *et al.*,[21] or Pt-TiN/Si_3N_4 nanocomposites which in our very recent study[22] showed enhanced catalytic performance for dehydrogenation of sodium borohydride in water. Therefore, polymer-derived amorphous SiAlN ceramics are expected to have an impact on catalytic processes as a transition or noble metal-free advanced material and be of significant interest for clean energy applications such as advanced hydrogen production, storage and transportation systems.

Acknowledgements

This work was partially supported by JSPS KAKENHI Grant Number JP20K05076. Dr Samuel Bernard and Prof. Yuji Iwamoto would like to thank CNRS who financially supported present work *via* the International Research Project (IRP) 'Ceramics materials for societal challenges'.

Notes and references

1 L. Zhang, M. Zhou, A. Wang and T. Zhang, Selective Hydrogenation over Supported Metal Catalysts: From Nanoparticles to Single Atoms, *Chem. Rev.*, 2020, **120**, 683–733.

2 F. Zaera, The Surface Chemistry of Metal-Based Hydrogenation Catalysis, *ACS Catal.*, 2017, **7**, 4947–4967.

3 J. M. Asensio, D. Bouzouita, P. W. N. M. Van Leeuwen and B. Chaudret, s-H-H, s-C-H, and s-Si-H Bond Activation Catalyzed by Metal Nanoparticles, *Chem. Rev.*, 2019, **120**, 1042–1084.

4 S. Kattel, P. Liu and J. G. Chen, Tuning Selectivity of CO_2 Hydrogenation Reactions at the Metal/Oxide Interface, *J. Am. Chem. Soc.*, 2017, **139**, 9739–9754.

5 R. M. Kellogg, Reversible metal-free hydrogen activation, *Chemtracts*, 2007, **19**, 152–156.

6 D. W. Stephan, The broadening reach of frustrated Lewis pair chemistry, *Science*, 2016, **354**, aaf7229.

7 T. A. Rokob, A. Hamza, A. Stirling, T. Soós and I. Pápai, Turning frustration into bond activation: A theoretical

mechanistic study on heterolytic hydrogen splitting by frustrated Lewis pairs, *Angew. Chem., Int. Ed.*, 2008, **47**, 2435–2438.

8 Q. Wang, Q. Sun, P. Jena and Y. Kawazoe, Potential of AlN nanostructures as hydrogen storage materials, *ACS Nano*, 2009, **3**, 621–626.

9 P. Strak, K. Sakowski, P. Kempisty, I. Grzegory and S. Krukowski, Adsorption of N_2 and H_2 at AlN(0001) Surface: Ab Initio Assessment of the Initial Stage of Ammonia Catalytic Synthesis, *J. Phys. Chem. C*, 2018, **122**, 20301–20311.

10 S. H. Lim and J. Lin, Ab initio study of the hydrogen chemisorption of single-walled aluminum nitride nanotubes, *Chem. Phys. Lett.*, 2008, **466**, 197–204.

11 J. Beheshtian, H. Soleymanabadi, M. Kamfiroozi and A. Ahmadi, The H 2 dissociation on the BN, AlN, BP and AlP nanotubes: A comparative study, *J. Mol. Model.*, 2012, **18**, 2343–2348.

12 M. Moradi and N. Naderi, First principle study of hydrogen storage on the graphene-like aluminum nitride nanosheet, *Struct. Chem.*, 2014, **25**, 1289–1296.

13 P. Colombo, G. Mera, R. Riedel and G. D. Sorarù, Polymer-derived ceramics: 40 Years of research and innovation in advanced ceramics, *J. Am. Ceram. Soc.*, 2010, **93**, 1805–1837.

14 S. Bernard, F. Chassagneux, M. P. Berthet, D. Cornu and P. Miele, Crystallinity, crystalline quality, and microstructural ordering in boron nitride fibers, *J. Am. Ceram. Soc.*, 2005, **88**, 1607–1614.

15 S. Koyama, H. Takeda, Y. Saito, Y. Sugahara and K. Kuroda, Preparation of AlN from poly(ethyliminoalane) via pyrolysis, *J. Mater. Chem.*, 1996, **6**, 1055–1058.

16 Y. Iwamoto, W. Völger, E. Kroke, R. Riedel, T. Saitou and K. Matsunaga, Crystallization Behavior of Amorphous Silicon Carbonitride Ceramics Derived from Organometallic Precursors, *J. Am. Ceram. Soc.*, 2001, **84**, 2170–2178.

17 M. C. Bechelany, C. Salameh, A. Viard, L. Guichaoua, F. Rossignol, T. Chartier, S. Bernard and P. Miele, Preparation of polymer-derived Si–B–C–N monoliths by spark plasma sintering technique, *J. Eur. Ceram. Soc.*, 2015, **35**, 1361–1374.

18 O. Majoulet, C. Salameh, M. E. Schuster, U. B. Demirci, Y. Sugahara, S. Bernard and P. Miele, Preparation, characterization, and surface modification of periodic mesoporous silicon-aluminum-carbon-nitrogen frameworks, *Chem. Mater.*, 2013, **25**, 3957–3970.

19 D. Fonblanc, D. Lopez-Ferber, M. Wynn, A. Lale, A. Soleilhavoup, A. Leriche, Y. Iwamoto, F. Rossignol, C. Gervais and S. Bernard, Crosslinking chemistry of poly(vinylmethyl-co-methyl)silazanes toward low-temperature formable preceramic polymers as precursors of functional aluminium-modified Si-C-N ceramics, *Dalton Trans.*, 2018, **47**, 14580–14593.

20 M. Zaheer, T. Schmalz, G. Motz and R. Kempe, Polymer derived non-oxide ceramics modified with late transition metals, *Chem. Soc. Rev.*, 2012, **41**, 5102.

21 D. Schumacher, M. Wilhelm and K. Rezwan, Porous SiOC monoliths with catalytic activity by in situ formation of Ni nanoparticles in solution-based freeze casting, *J. Am. Ceram. Soc.*, 2020, **103**, 2991–3001.

22 A. Lale, M. D. Mallmann, S. Tada, A. Bruma, S. Özkar, R. Kumar, M. Haneda, R. A. Francisco Machado, Y. Iwamoto, U. B. Demirci and S. Bernard, Highly active, robust and reusable micro-/mesoporous TiN/Si_3N_4 nanocomposite-based catalysts for clean energy: Understanding the key role of TiN nanoclusters and amorphous Si_3N_4 matrix in the performance of the catalyst system, *Appl. Catal., B*, 2020, **272**, 118975.

23 R. S. Mikhail, S. Brunauer and E. E. Bodor, Investigations of a complete pore structure analysis. I. Analysis of micropores, *J. Colloid Interface Sci.*, 1968, **26**, 45–53.

24 E. P. Barrett, L. G. Joyner and P. P. Halenda, The Determination of Pore Volume and Area Distributions in Porous Substances. I. Computations from Nitrogen Isotherms, *J. Am. Chem. Soc.*, 1951, **73**, 373–380.

25 M. Schmid, H. P. Steinrück and J. M. Gottfried, A new asymmetric Pseudo-Voigt function for more efficient fitting of XPS lines, *Surf. Interface Anal.*, 2014, **46**, 505–511.

26 K. S. W. Sing, D. H. Everett, R. A. W. Haul, L. Moscou, R. A. Pierotti, J. Rouquerol and T. Siemieniewska, Reporting Physisorption Data for Gas/Solid Systems with Special Reference to the Determination of Surface Area and Porosity, *Pure Appl. Chem.*, 1985, **57**, 603–619.

27 S. Lowell, J. E. Shields, M. A. Thomas and M. Thommes, *Characterization of Porous Solids and Powders: Surface Area, Pore Size and Density*, Springer, Dordrecht, 2004, pp. 129– 156.

28 C. Schitco, M. S. Bazarjani, R. Riedel and A. Gurlo, NH_3-assisted synthesis of microporous silicon oxycarbonitride ceramics from preceramic polymers: A combined N_2 and CO_2 adsorption and small angle X-ray scattering study, *J. Mater. Chem. A*, 2015, **3**, 805–818.

29 S. Duperrier, C. Gervais, S. Bernard, D. Cornu, F. Babonneau and P. Miele, Controlling the chemistry, morphology and structure of boron nitride-based ceramic fibers through a comprehensive mechanistic study of the reactivity of spinnable polymers with ammonia, *J. Mater. Chem.*, 2006, **16**, 3126–3138.

30 G. Petzow and R. Sersale, Characterization of Si_3N_4 powders, *Pure Appl. Chem.*, 1987, **59**, 1673–1680.

31 K. Yamamoto, Y. Koga and S. Fujiwara, Binding Energies of Amorphous CN and SiCN Films on X-Ray Photoelectron Spectroscopy, *Jpn. J. Appl. Phys.*, 2001, **40**, L123–L126.

32 L. Rosenberger, R. Baird, E. McCullen, G. Auner and G. Shreve, XPS analysis of aluminum nitride films deposited by plasma source molecular beam epitaxy, *Surf. Interface Anal.*, 2008, **40**, 1254–1261.

33 Y. Li, W. Zhang, L. Zhang, Q. Yang, Z. Wei, Z. Feng and C. Li, Direct Synthesis of Al—SBA-15 Mesoporous Materials via Hydrolysis-Controlled Approach, *J. Phys. Chem. B*, 2004, **108**, 9739–9744.

34 R. J. Madix, The application of flash desorption spectroscopy to chemical reactions on surfaces: Temperature

programmed reaction spectroscopy, *Crit. Rev. Solid State Mater. Sci.*, 1978, **7**, 143–152.

35 E. Tal-Gutelmacher, D. Eliezer and E. Abramov, Thermal desorption spectroscopy (TDS)-Application in quantitative study of hydrogen evolution and trapping in crystalline and non-crystalline materials, *Mater. Sci. Eng., A*, 2007, **445–446**, 625–631.

36 G. Verdecia, K. L. O'Brien, W. R. Schmidt and T. M. Apple, Aluminum-27 and Silicon-29 Solid-State Nuclear Magnetic Resonance Study of Silicon Carbide/Aluminum Nitride Systems: Effect of Silicon/Aluminum Ratio and Pyrolysis Temperature, *Chem. Mater.*, 1998, **10**, 1003–1009.

37 Z. Xiong, G. Wu, J. Hu, Y. Liu, P. Chen, W. Luo and J. Wang, Reversible hydrogen storage by a Li-AI-N-H complex, *Adv. Funct. Mater.*, 2007, **17**, 1137–1142.

38 F. Cheng, S. M. Kelly, F. Lefebvre, S. Clark, R. Supplit and J. S. Bradley, Preparation of a mesoporous silicon aluminium nitride via a non-aqueous sol-gel route, *J. Mater. Chem.*, 2005, **15**, 772–777.

39 Y. Ren, O. Jiang, H. Zeng, Q. Mao and H. Jiang, Lewis acid-base bifunctional aluminum-salen catalysts: synthesis of cyclic carbonates from carbon dioxide and epoxides, *RSC Adv.*, 2016, **6**, 3243–3249.

40 J. Haase, D. Freude, T. Fröhlich, G. Himpel, F. Kerbe, E. Lippmaa, H. Pfeifer, P. Sarv, H. Schäfer and B. Seiffert, ^{27}Al magic-angle-spinning NMR studies of aluminum nitride ceramics, *Chem. Phys. Lett.*, 1989, **156**, 328–332.

41 A. Haaland, Covalent versus Dative Bonds to Main Group Metals, a Useful Distinction, *Angew. Chem., Int. Ed. Engl.*, 1989, **28**, 992–1007.

42 E. Magnusson, Hypercoordinate Molecules of Second-Row Elements: D Functions or d Orbitals, *J. Am. Chem. Soc.*, 1990, **112**, 7940–7951.

43 W. L. Nelson and C. J. Engelder, The Thermal Decomposition of Formic Acid, *J. Phys. Chem.*, 1926, **30**, 470–475.

44 T. Meisel, Z. Halmos, K. Seybold and E. Pungor, The thermal decomposition of alkali metal formates, *J. Therm. Anal.*, 1975, **7**, 73–80.

Supplementary Information

Novel hydrogen chemisorption properties of amorphous ceramic compounds consisting of *p*-block elements: exploring Lewis acid-base Al–N pair site formed *in-situ* within polymer-derived silicon-aluminum-nitrogen-based system

Shotaro Tada,[a] Norifumi Asakuma,[a] Shiori Ando,[a] Toru Asaka,[a] Yusuke Daiko,[a] Sawao Honda,[a] Masaaki Haneda,[a] Samuel Bernard,[b] Ralf Riedel[c] and Yuji Iwamoto*[a]

[a]Department of Life Science and Applied Chemistry, Graduate School of Engineering, Nagoya Institute of Technology, Gokiso-cho, Showa-ku, Nagoya 466-8555, Japan
[b]University of Limoges, CNRS, IRCER, UMR 7315, F-87000, Limoges, France
[c]Institut für Materialwissenschaft, Technische Universität Darmstadt, Otto-Berndt-Str. 3, 64287 Darmstadt, Germany

* Corresponding author: Yuji Iwamoto
E-mail: iwamoto.yuji@nitech.ac.jp
Tel/Fax: +81-52-735-5276

Keywords:
Polymer-Derived Ceramics (PDCs) / amorphous SiAlN / Molecular hydrogen (H_2) chemisorption / CO_2 hydrogenation reactions / Lewis acid-base pair site

In this study, aluminum (Al)-modified polysilazane, as a single-source precursor, was first synthesized by chemical modification of a commercially available Durazane® 1800, poly(vinylmethyl-co-methyl)silazane (PSZ, silicon nitride precursor) with alane *N*,*N*-dimethylethylamine ($EtNMe_2 \cdot AlH_3$—ADMEA). The reaction of PSZ and ADMEA relies on both dehydrocoupling and hydroalumination reactions (Fig. S1).

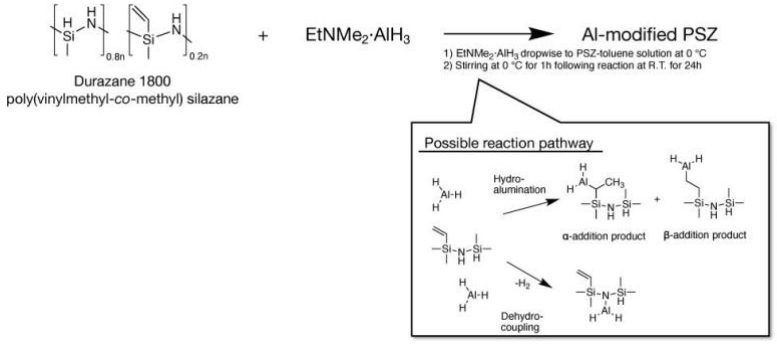

Fig. S1 Schematic representation of the synthesis of Al-modified PSZ through PDCs route.

The chemical modification performed in this study was monitored by attenuated total reflection flourier transform infra-red (ATR-FTIR) spectroscopy using FTIR spectrometer (FT/IR-4200IF, JASCO Corporation, Tokyo, Japan) with attachment of ATR equipment (ATR PRO 550S-S/570S-H, JASCO Corporation, Tokyo, Japan) at a resolution of 4 cm^{-1}. The typical ATR-FTIR spectra of Al-PSZ samples with different Al/Si atomic ratios shows in Fig. S2. The FT-IR spectra shows that the intensity of the bands corresponding to the C_{sp2}–H band at 3048 and 1402 cm^{-1} slightly reduces. In parallel, the intensity of the bands assigned to N–H bands at 3381 and 1173 cm^{-1} reduces more significantly. These changes indicate both hydroalumination and dehydrocoupling reaction occur in parallel. FTIR (ATR/cm^{-1}): ν(N–H) = 3350 (m); ν(C_{sp2}–H) = 3048 (w); ν(C_{sp3}–H) = 2950 (m), 2900 (vw); ν(Si–H) = 2130 (vs); ν(Al–H) = 1820 (m); ν(C=C) = 1596 (vw); δ(C–C, vinyl) = 1402 (w); δ(Si–CH_3) = 1250 (vs); δ(Si_2N–H) = 1175 (vs); δ(Si–N) = 840–1020 (vs); and δ(Si–C) = 700–850 (m).

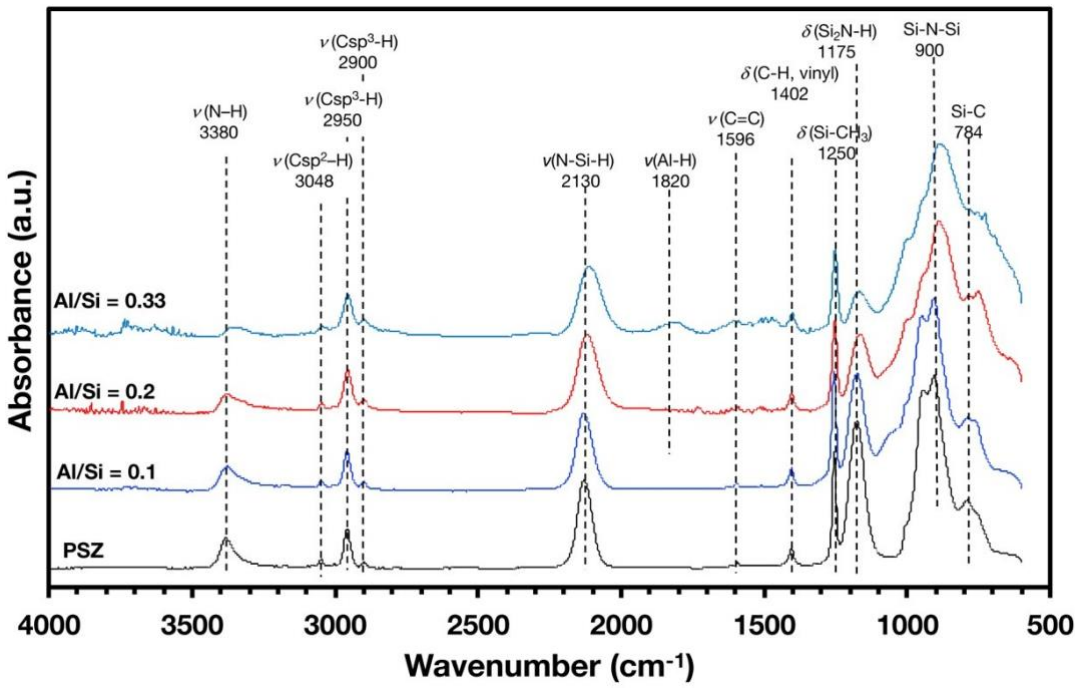

Fig. S2 ATR-FT-IR spectra for as-received PSZ and Al-modified PSZ.

In this study, Al-PSZ was pyrolyzed at 1000 °C under flowing ammonia (NH_3) to generate a silicon-aluminum-nitrogen-based ceramic. Powder X-ray diffraction (XRD) patterns of the pyrolyzed samples were measured on a flat sample stage, using Ni-filtered CuK□ radiation (Model X'pert, Philips, Amsterdam, The Netherlands). The XRD patterns of as-pyrolyzed samples are shown in Fig. S3. The XRD pattern of as-pyrolyzed SiAlN (**SiAlN**) is X-ray amorphous and does not show any difference with the Al-free sample, *i.e.*, the as-pyrolyzed silicon nitride (**SiN**) sample, prepared through the same pyrolysis procedure.

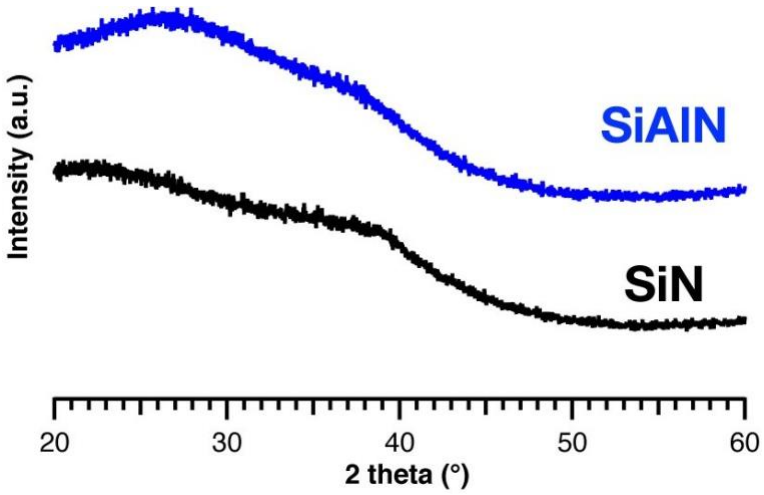

Fig. S3 Typical XRD patterns of samples after pyrolysis at 1000 °C under flowing NH_3.

Textural properties of pyrolyzed samples was evaluated by measuring N_2 adsorption and desorption isotherms at –196 °C under the relative pressures ranging from 0 to 0.99 (Model Belsorp Max, BEL Japan Inc., Osaka, Japan). The pore size distribution was analyzed by MP[1] and BJH[2] methods. The results are shown in Fig. S4. The **SiAlN** sample at –196 °C exhibited a type I+IV isotherms according to the IUPAC classifications[3, 4], while the **SiN** sample showed no interaction with N_2 (Fig. S4a). The Brunauer-Emmett-Teller (BET) surface area ($S_{BET}^{N_2}$) of the **SiAlN** sample has been measured to be 165 $m^2\,g^{-1}$. The pore size distribution curve (PSD) in the micropore range characterized by the MP meshod[1] exhibited a peak centered at 1.2 nm (Fig. S4b), whereas there was no distinct peak in the mesopore range by the BJH plot[2] although we can identify the existence of a certain porosity with a pore size range of approximately 2 to 4 nm (Fig. S4c). In addition, Fig. S5 shows a N_2 adsorption and desorption isotherm of the

SiAlN sample pyrolyzed at 700 °C which has low porosity due to the collapse and close of the pore.

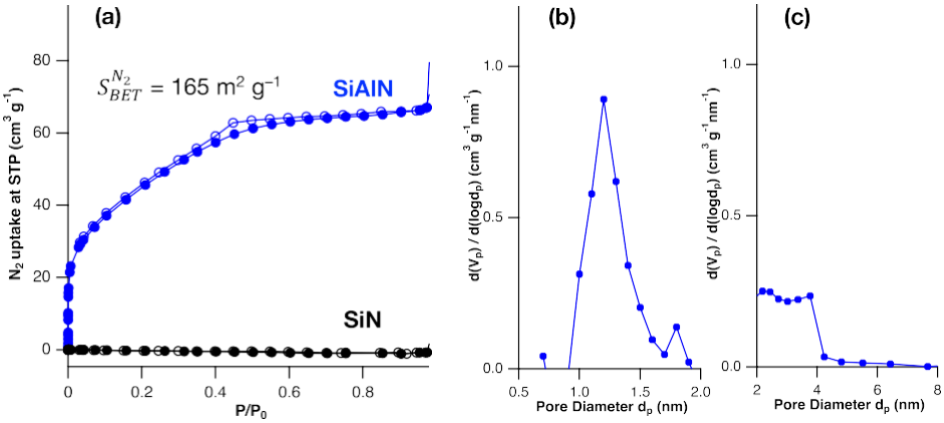

Fig. S4 (a) N_2 adsorption-desorption isotherms at –196 °C for the polymer-derived amorphous **SiAlN** and **SiN** samples, and pore size distribution curves of the SiAlN sample characterized by (b) MP plot and (c) BJH plot.

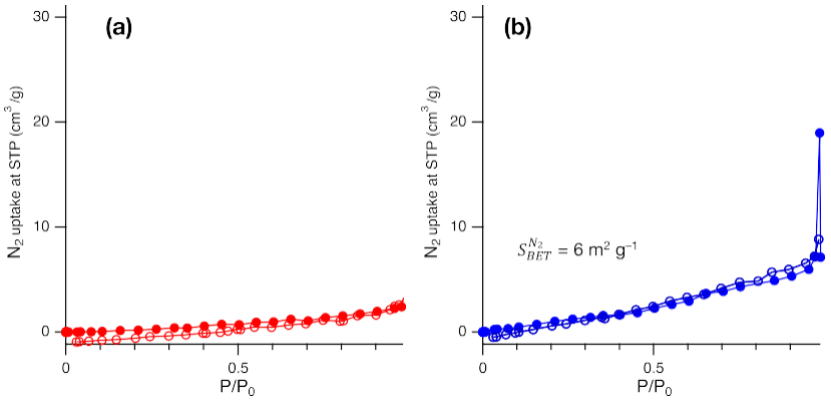

Fig. S5 Reference data of N_2 adsorption and desorption isotherms at –196 °C. Polymer-derived SiAlN pyrolyzed (a) at 1000 °C under N_2 and (b) at 700 °C under NH_3 .

Thermalgravimetric (TG) analysis for the polymer-to-ceramic conversion was performed under flowing mixture of NH_3 and N_2 (60:40 in flow ratio) (Model TGA 92 16.18 Setaram, Inc., Newark, CA, USA) or He (Model JMS-Q1500GC, JEOL Ltd., Tokyo, Japan). The TG-curves under the mixed NH_3-N_2 gas flow were monitored up to 1000 °C with a heating rate of 5 °C min^{-1} (Fig. S6), while those under He flow were monitored up to 1000 °C with a heating rate of 10 °C min^{-1} (Fig. S7).

A contentious weight loss above 700 °C is identified during the conversion of the Al-modified PSZ leading to the **SiAlN** sample whereas no weight loss is identified above 800 °C during the conversion of PSZ into the SiN sample (Fig. S6), in contrast, such the difference

above 800 °C is not observed when the conversions of Al-modified PSZ and PSZ were monitored under He (Fig. S7).

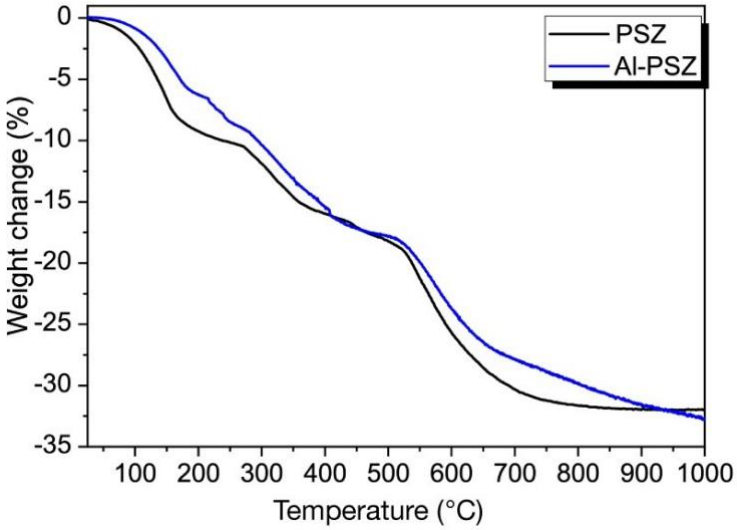

Fig. S6 TG-curves of PSZ and Al-PSZ under flowing NH_3-N_2 (60:40 in flow ratio) mixed gas.

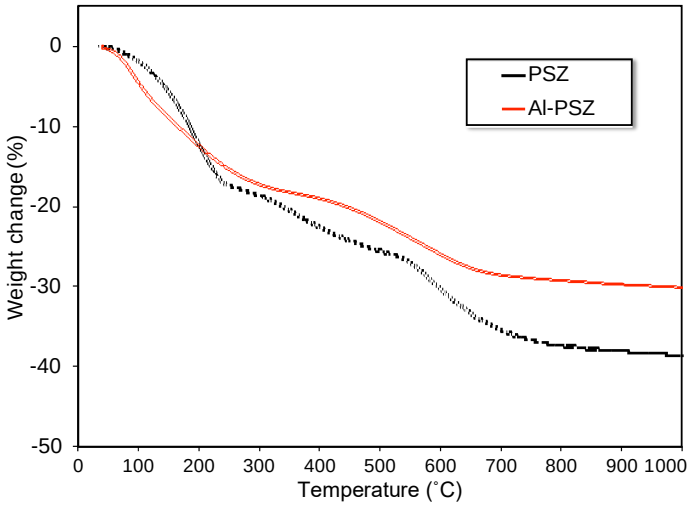

Fig. S7 TG-curves of PSZ and Al-PSZ under flowing He.

To investigate the chemical bonding-state of the **SiAlN** sample, X-ray photoelectron spectroscopic (XPS) measurements were performed using X-ray Photoelectron Spectrometer (PHI 5000, ULVAC-PHI, Inc., Japan) with an Al K*a* X-ray source operated at 14 kV and 14 mA. An alignment on the C 1s peak was performed before survey scans. The wide scan spectrum of **SiAlN** sample is shown in Fig. S8. Besides the intense lines of the constituent elements (N 1s, Si 2p and Al 2p) and unavoidable carbon contaminant, strong line of O 1s is observed. This indicates a certain amount of oxygen is present at the surface of the **SiAlN** sample. The summary of XPS characterization for amorphous SiAlN sample lists in Table S2.

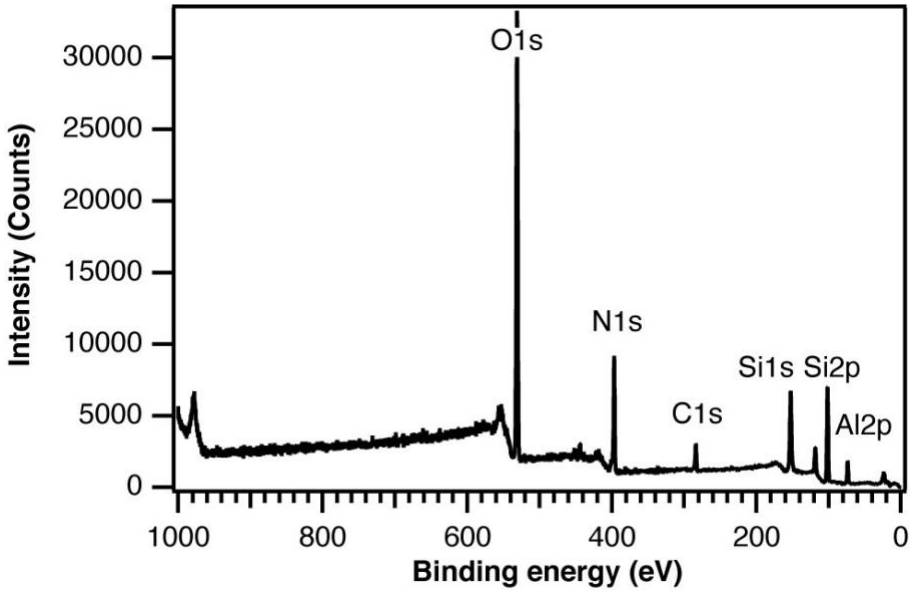

Fig. S8 Wide scan x-ray photoelectron spectrum of polymer-derived SiAlN.

Table S1 Summary of XPS characterization for amorphous SiAlN sample. (a) Al 2p and (b) Si 2p.

(a)

Band (Al 2p)	Binding energy (eV)	Area (%)
Al-N	73.5	78.0
Al-O	74.7	22.0

(b)

Band (Si 2p)	Binding energy (eV)	Area (%)
Si-N	73.5	98.8
Si-O	74.7	1.2

To study the H_2 adsorption and desorption properties, temperature-programmed-desorption of hydrogen (H_2-TPD) was performed using a catalyst analyzer (Model BELCAT-A, MicrotracBEL Corp., Osaka, Japan) fixed with a quadrupole mass spectrometer (Model BELMASS, MicrotracBEL Corp., Osaka, Japan). Prior to the measurement, the sample was maintained under Ar at 800 °C and subsequently exposed to H_2 at specific temperatures (T_{H2} = 100, 150 °C) for 5 min. H_2-TPD profiles of the reference samples are shown in Fig. S9. The amorphous silicon nitride which is derived from the as-received PSZ, commercial crystalline AlN and HY zeolite samples show no desorption peak under the measurement condition (T_{H2} = 150 °C), while the H_2-TPD profiles of the ***H₂PTSiAlN*** sample exhibits a single peak at approximately 100 to 350 °C under the same condition (T_{H2} = 150 °C). As referential data, the volumetric amount of hydrogen desorption briefly estimated for the ***H₂PTSiAlN*** sample is approximately 1.1 mL g^{-1} which was calculated based on the relative ratio of the peak area of H2-TPD curve, T_{H2} = 150 °C in Fig. S9, to that of well-known metal hydride, MgH_2 measured at our lab.

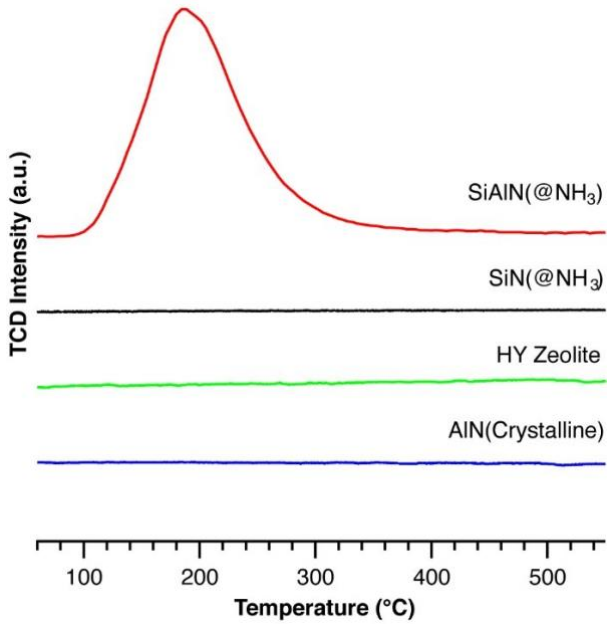

Fig. S9 Comparison of H_2-TPD profiles of **PTSiAlN** sample with those of reference samples of **SiN** sample, commercially available crystalline AlN and zeolite samples.

References

1. R. S. Mikhail, S. Brunauer and E. E. Bodor, Investigations of a complete pore structure analysis. I. Analysis of micropores, *J. Colloid Interface Sci.*, 1968, **26**, 45–53.
2. E. P. Barrett, L. G. Joyner and P. P. Halenda, The Determination of Pore Volume and Area Distributions in Porous Substances. I. Computations from Nitrogen Isotherms, *J. Am. Chem. Soc.*, 1951, **73**, 373–380.
3. K. S. W. Sing, D. H. Everett, R. A. W. Haul, L. Moscou, R. A. Pierotti, J. Rouquerol and T. Siemieniewska, Reporting Physisorption Data for Gas/Solid Systems with Special Reference to the Determination of Surface Area and Porosity, *Pure Appl. Chem.*, 1985, **57**, 603–619.
4. S. Lowell, J. E. Shields, M. A. Thomas and M. Thommes, Springer, Dordrecht, 2004, pp. 129–156.